

Anti-allodynic effect of 2-(aminomethyl)adamantane-1-carboxylic acid in a rat model of neuropathic pain: A mechanism dependent on Ca_v2.2 channel inhibition



Grigoris Zoidis^{a,*}, Alejandro Sandoval^b, Jorge Baruch Pineda-Farias^c, Vinicio Granados-Soto^c, Ricardo Felix^{d,*}

^a Faculty of Pharmacy, Department of Pharmaceutical Chemistry, University of Athens, Panepistimioupoli-Zografou, GR-15771 Athens, Greece

^b School of Medicine FES Iztacala, National Autonomous University of Mexico (UNAM), Tlalnepantla, Mexico

^c Departamento de Farmacobiología, Centro de Investigación y de Estudios Avanzados (Cinvestav), Sede Sur., México, D.F., Mexico

^d Department of Cell Biology, Cinvestav, Mexico City, Mexico

ARTICLE INFO

Article history:

Received 1 November 2013

Revised 29 January 2014

Accepted 7 February 2014

Available online 15 February 2014

Keywords:

Allodynia
Calcium channels
Neuropathic pain
Gabapentin

ABSTRACT

Neuropathic pain is a serious physical disabling condition resulting from lesion or dysfunction of the peripheral sensory nervous system. Despite the fact that the mechanisms underlying neuropathic pain are poorly understood, the involvement of voltage-gated calcium (Ca_v) channels in its pathophysiology has justified the use of drugs that bind the Ca_v channel $\alpha_2\delta$ auxiliary subunit, such as gabapentin (GBP), to attain analgesic and anti-allodynic effects in models involving neuronal sensitization and nerve injury. GBP binding to $\alpha_2\delta$ inhibits nerve injury-induced trafficking of the α_1 pore forming subunits of Ca_v channels, particularly of the N-type, from the cytoplasm to the plasma membrane of pre-synaptic terminals in dorsal root ganglion neurons and dorsal horn spinal neurons. In the search for alternative forms of treatment, in this study we describe the synthesis and pharmacological profile of a GABA derivative, 2-aminoadamantane-1-carboxylic acid (**GZ4**), which displays a close structure–activity relationship with GBP. Behavioral assessment using von Frey filament stimuli showed that **GZ4** treatment reverted mechanical allodynia/hyperalgesia in an animal model of spinal nerve ligation-induced neuropathic pain. In addition, using the patch clamp technique we show that **GZ4** treatment significantly decreased whole-cell currents through N-type Ca_v channels heterologously expressed in HEK-293 cells. Interestingly, the behavioral and electrophysiological time course of **GZ4** actions reflects that its mechanism of action is similar but not identical to that of GBP. While GBP actions require at least 24 h and imply uptake of the drug, which suggests that the drug acts mainly intracellularly affecting channels trafficking to the plasma membrane, the faster time course (1–3 h) of **GZ4** effects suggests also a direct inhibition of Ca²⁺ currents acting on cell surface channels.

© 2014 Elsevier Ltd. All rights reserved.

1. Introduction

Neuropathic pain is an important clinical problem that drastically impairs the quality of life of patients. This condition is manifested as tactile allodynia (a painful sensation to a non-noxious stimulus) and or hyperalgesia (an enhanced sensation to a painful stimulus). Neuropathic pain may be caused by nerve injury and is

usually accompanied by a painful sensation that is only partially relieved by analgesics.

It is well acknowledged that certain groups of sensory neurons are the main mediators of pain sensation. Sensory neurons transmit information from the periphery to the spinal cord which then transfers this information to the brainstem and forebrain. Though the molecular basis underlying neuropathic pain are not well understood, nerve damage may cause hyperexcitability by increasing the firing frequency and/or generation of spontaneous action potentials from dorsal root ganglion (DRG) neurons.¹

High-threshold N-type (Ca_v2.2) voltage-gated Ca²⁺ channels, which transduce electrical activity into other cellular functions, regulate Ca²⁺ homeostasis and are thought to play a major role in processing pain information.² The function and distribution of

* Corresponding authors. Addresses: Faculty of Pharmacy, Department of Pharmaceutical Chemistry, University of Athens, Panepistimioupoli-Zografou, GR-15771 Athens, Greece. Tel.: +30 210 7274809 (G.Z.), Departamento de Biología Celular, Cinvestav-IPN, Avenida IPN #2508, Colonia Zacatenco, México, D.F. CP 07300, Mexico. Tel.: +52 55 57 47 39 88 (R.F.).

E-mail addresses: zoidis@pharm.uoa.gr (G. Zoidis), rfelix@cell.cinvestav.mx (R. Felix).

these channels may vary among different types of neurons, however they are predominantly expressed in nerve terminals, where they control neurotransmitter release. Indeed, genetic and pharmacological studies have revealed that N-type channels are important for pain sensation in disease models.² These data suggest that N-type channel inhibitors or modulators could be developed into useful drugs to treat neuropathic pain.³

In a recent report, we described the synthesis and pharmacological profile of a GABA adamantane derivative (AdGABA), which displayed a close structure-activity relationship with gabapentin (GBP).⁴ Since GBP has been shown to reduce the functional expression of neuronal N-type ($\text{Ca}_v2.2$) channels,^{5,6} we examined the consequences of the AdGABA treatment on membrane neuronal recombinant $\text{Ca}_v2.2$ channels. Our results showed an alteration in $\text{Ca}_v2.2$ channel functional expression after chronic treatment with AdGABA presumably caused by a direct interaction of the drug on the $\alpha_2\delta$ auxiliary subunit of the channels. However, AdGABA may not bind to the same site as GBP in $\alpha_2\delta$.⁷

To obtain further insight into how structural features may affect the anti-nociceptive activity of compounds based on γ -aminobutyric acid that modulate N-type Ca^{2+} channels, here we explored the biological effect of the 2-(aminomethyl)adamantane-1-carboxylic acid (**GZ4**). In this compound part of the γ -aminobutyric acid pharmacophore was introduced to the adamantane carbon skeleton (Fig. 1A). As we reported previously, GBP and AdGABA show similarities in the orientation in both the carboxymethylene and aminomethylene moiety. However, in the case of **GZ4** the carboxylic acid group possessed a different orientation (Fig. 1B). As we shall discuss later, these results might explain some differences in the mode of action of these compounds. Last, but not least, data from behavioral testing showed that intrathecal application of **GZ4** significantly reversed nerve ligation-induced tactile allodynia in a rat model of neuropathic pain.

2. Experimental

2.1. Chemistry

2.1.1. General

Melting points were determined using a Büchi capillary apparatus and are uncorrected. IR spectra were recorded on a Perkin-Elmer 833 photometer. The ^1H and ^{13}C NMR spectra were obtained on either a Bruker MSL 400 (400 MHz ^1H ; 100 MHz ^{13}C) or Bruker 600 (600 MHz ^1H) spectrometer, using CDCl_3 or $\text{DMSO}-d_6$ as

solvent. Chemical shifts are reported in δ (ppm) with the tetramethylsilane or solvent ($\text{DMSO}-d_6$) as internal standard. Splitting patterns are designated as s, singlet; d, doublet; dd, doublet of doublets; t, triplet; td, triplet of doublets; q, quartet; m, multiplet; br, broad; v br, very broad; sym, symmetrical. Coupling constants (J) are expressed in units of hertz (Hz). The spectra were recorded at 293 K (20 °C) unless otherwise specified. Carbon multiplicities were established by DEPT experiments. The 2D NMR experiments (HMQC and COSY) were performed for the elucidation of the structures of the newly synthesized compounds.

Analytical thin-layer chromatography (TLC) was conducted on precoated Merck silica gel 60 F_{254} plates (layer thickness 0.2 mm) with the spots visualized by iodine vapors and/or UV light. Column chromatography purification was carried out on silica gel 60 (70–230 mesh). Elemental analyses (C, H, N) were performed by the *Service Central de Microanalyse* at CNRS (France), and were within $\pm 0.4\%$ of the theoretical values. Elemental analysis results for the tested compound correspond to >95% purity. The commercial reagents were purchased from Alfa Aesar, Sigma–Aldrich, and Merck. Organic solvents used were in the highest purity, and when necessary, were dried by standard methods. Solvent abbreviations: DME, dimethoxyethane; Et_2O , ethyl ether; MeOH, methanol; EtOH, ethanol; AcOEt, ethyl acetate; DMSO, dimethylsulfoxide.

2.1.1.1. Methyl(2-oxotricyclo[3.3.1.1^{3,7}]decane-1-carboxylate **5**

A mixture of the acid **4** (1.08 g, 5.6 mmol) and thionyl chloride (4 mL) was heated at 65 °C for 15 min. The excess thionyl chloride was removed under vacuum, and the resulting chloride was esterified in a methanolic solution (20 mL) to give, after 1 h at room temperature (RT) and 0.5 h at 70 °C, 1.14 g (quantitative yield) of methylester **5** as a white solid; mp = 86–88 °C; IR (mull) ν 1731 cm^{-1} (CO), 1711 cm^{-1} (CO); ^1H NMR (400 MHz, CDCl_3) δ 1.57–1.96 (complex m, 7H, 4e, 6, 8a, 9e, 10-H), 2.00–2.06 (m, 4H, 4a, 5, 7, 8e-H), 2.12 (d, 1H, J = 12.0, 9a-H), 3.69 (s, 3H, CO_2CH_3) ppm; ^{13}C NMR (100 MHz, CDCl_3) δ 26.7 (5-C), 26.8 (7-C), 30.8 (3-C), 32.1 (4-C), 34.0 (9-C), 35.7 (8, 10-C), 39.4 (6-C), 42.7 (1-C), 61.1 (COOCH_3), 174.4 (C=O), 217.4 (2-C) ppm. Anal. Calcd for $\text{C}_{12}\text{H}_{16}\text{O}_3$: C, 69.21; H, 7.74. Found: C, 69.34; H, 7.68.

2.1.1.2. Methyl 2-cyanotricyclo[3.3.1.1^{3,7}]decane-1-carboxylate **6**

Solid *t*-BuOK (0.60 g, 4.3 mmol) was added portion wise to a stirred (argon atmosphere) solution of ketoester **5** (0.48 g, 2.31 mmol) and TosMIC (0.55 g, 2.8 mol) in a mixture of 8 mL of DME and 0.3 mL of absolute EtOH maintained at 5–10 °C. The cooling was removed and stirring continued for 30 min and the mixture was then heated (48 °C) for 60 min. The suspension obtained was cooled to RT with stirring. The precipitate (TosK) was filtered and washed with DME. The combined DME solutions were concentrated and purified by flashing the concentrate over silica gel using as eluents *n*-pentane– Et_2O (3:1) to afford cyanoester **6** (410 mg, 81%); mp 55–57 °C (*n*-hexane); IR (mull) ν 2237 cm^{-1} (CN), 1728 cm^{-1} (CO); ^1H NMR (400 MHz, CDCl_3) δ (ppm) 1.69–2.16 (m, 12H, 4, 5, 6, 7, 8, 9, 10-H), 2.28 (d, 1H, J = 2.7 Hz, 3-H), 3.19 (d, 1H, J = 2.7 Hz, 2-H), 3.72 (s, 3H, CH_3) ppm; ^{13}C NMR (100 MHz, CDCl_3) δ 26.8 (5-C), 26.9 (7-C), 30.8 (3-C), 32.3 (4-C), 34.2 (9-C), 35.6 (8, 10-C), 38.1 (2-C), 39.4 (6-C), 42.8 (1-C), 120.6 (CN), 174.6 (C=O). Anal. Calcd for $\text{C}_{12}\text{H}_{15}\text{NO}_2$: C, 70.22; H, 7.37. Found: C, 70.39; H, 7.62.

2.1.1.3. 2-Cyanotricyclo[3.3.1.1^{3,7}]decane-1-carboxylic acid **7**

A solution of the cyanoester **6** (9.37 g, 42.8 mmol) in ethanol (50 mL) was added to a solution of NaOH (3.03 g, 75 mmol) in water (20 mL), the flask was stoppered and left standing at RT for 48 h. After evaporation of the solvent the precipitated salt was dissolved in warm water. The solution was chilled in an ice bath and acidified with concentrated HCl. The precipitated solid was filtered

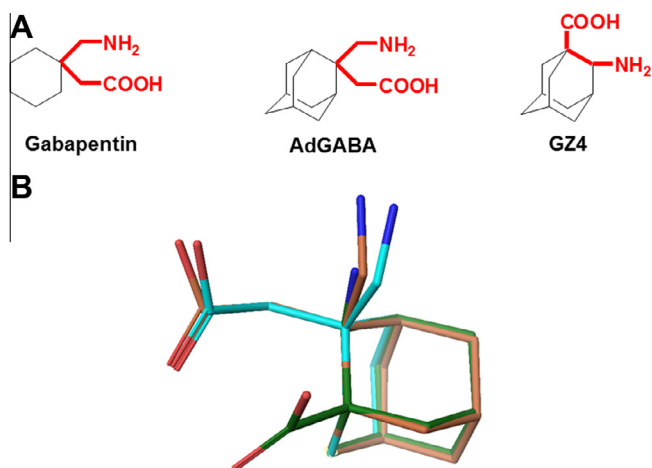


Figure 1. Gabapentin and gabapentinoid drugs. (A) Structural comparison of the antiepileptic/antinociceptive gabapentin, AdGABA and compound **8** (GZ4). (B) Superposition of gabapentin (blue), AdGABA (pink) and compound GZ4 (green).

off, washed with water and dried: yield 8.16 g (93% from the cyanoester **6**); mp 160–162 °C (Et₂O–*n*-pentane); IR (mull) ν 2234 cm⁻¹ (CN), 1707 cm⁻¹ (C=O); ¹H NMR (400 MHz, CDCl₃), δ 1.67–1.72 (m, 4H, 4e, 6, 8a-H), 1.83–1.94 (m, 2H, 8a, 10a-H), 2.00–2.13 (m, 5H, 4a, 5, 7, 8e, 10e, 9e-H), 2.14–2.22 (br d, 1H, 9a-H), 2.32 (d, 1H, *J* = 2.0 Hz, 3-H), 3.19 (s, 1H, 2-H), 9.88 (br s, COOH) ppm; ¹³C NMR (CDCl₃, 100 MHz), δ 26.6 (7-C), 26.7 (5-C), 30.8 (3-C), 32.0 (4-C), 33.8 (9-C), 35.6 (6, 8-C), 38.1 (2-C), 39.3 (10-C), 42.8 (1-C), 120.5 (C≡N), 180.8 (C=O) ppm. Anal. Calcd for C₁₂H₁₅NO₂: C, 70.22; H, 7.36. Found: C, 70.39; H, 7.62.

2.1.1.4. 2-Aminomethyl-1-tricyclo[3.3.1.1^{1,7}]decanecarboxylic acid hydrochloride **GZ4**.

A solution of cyanoacid **7** (6.5 g, 31.7 mmol) in absolute ethanol (50 mL) and HCl (37%, 5 mL) was hydrogenated in the presence of PtO₂ (1 g) catalyst under a pressure of 50 psi, at 25 °C, for 5 h. A white solid was formed, which was dissolved in methanol. The suspension was filtered to remove the catalyst and the filtrate was evaporated until a small volume remained. Dry ether was then added and the mixture was chilled. The amino acid hydrochloride **8** solid formed, was filtered and washed with dry ether: yield 6.43 g (almost quantitative); mp 204–206 °C (dec., MeOH–Et₂O), IR (Nujol) ν (C=O) 1717 cm⁻¹; ¹H NMR (400 MHz, DMSO-*d*₆), δ 1.42 (d, 1H, *J* = 12.8 Hz, 4e-H), 1.55–1.86 (complex m, 9H, 4a, 6, 8, 9, 10-H), 1.88 (br s, 1H, 7-H), 1.95 (br s, 1H, 3-H), 2.03 (br s, 1H, 5-H), 2.20 (br d, 1H, *J* = 10.8 Hz, 2-H), 2.57 (dd, 1H, *J* = 12.4 and 2.8 Hz, CH_AH_MNH₂-HCl), 2.95 (t, 1H, *J* = 12.0 Hz, CH_AH_MNH₂-HCl), 8.14 (br s, NH₂), 12.51 (br s, COOH) ppm; ¹³C NMR (CDCl₃, 100 MHz), δ 26.8 (7-C), 26.9 (5-C), 27.1 (3-C), 29.5 (4-C), 32.3 (9-C), 36.2 (6-C), 37.0 (8-C), 38.2 (CH₂NH₂Cl), 41.2 (10-C), 42.3 (1-C), 42.7 (2-C), 177.4 (C=O) ppm. Anal. Calcd for C₁₂H₂₀ClNO₂: C, 58.65; H, 8.20. Found: C, 58.89; H, 8.54.

2.2. Biology

2.2.1. Spinal nerve ligation-induced neuropathic pain model and measurement of tactile allodynia

Sprague Dawley rats (140–160 g) were housed in cages on a standard 12/12 h light/dark cycle and had free access to food and drinking water before experiments. All experiments were performed according to the Guidelines on Ethical Standards for Investigation of Experimental Pain in Animals⁸ and the Mexican regulation (NOM-062-ZOO-1999). In addition, these experiments were approved by our local Ethics Committee (Protocol 455, Cinvestav).

Spinal nerve ligation was produced in animals as follows. Intraperitoneal injection of ketamine/xylazine (45:12 mg/kg) was used to anesthetize the rats. The back skin of the animals was shaved and prepared aseptically for surgery. A midline incision was made at the dorsal region followed by a blunt dissection to expose the corresponding spinal cord region. The left L5 and L6 spinal nerves were exposed and ligated with suture distal to the dorsal root ganglion. In the sham group, the surgical procedure was identical, but the spinal nerves were not ligated. Rats were allowed to recover for 9 d before a second surgery to implant an intrathecal catheter. For this procedure, animals were anesthetized with a ketamine/xylazine (45:12 mg/kg, i.p.) and placed in a stereotaxic head holder to expose the atlantooccipital membrane.⁹ A PE-10 catheter was then passed intrathecally to the level of the lumbar junction. Rats were allowed to recover from surgery for 5 d. Animals showing signs of motor impairment were excluded from the studies and euthanized.

Development of tactile allodynia was determined using the 50% withdrawal threshold method (PWT) as described previously.¹⁰ Sham and spinal nerve ligated rats were placed in individual clear chambers positioned on top of a mesh screen for 30–40 min acclimation. A series of von Frey filaments were then used to measure

the degree of mechanical sensitivity based on the up–down method described by Dixon (1980).¹¹ Each filament was applied in a perpendicular fashion to the glabrous plantar surface of each hind paw with a force causing the filament to buckle. This degree of force was maintained for 5 s or until a positive response in the form of sharp withdrawal or paw licking was observed. No withdrawal response prompted the use of next filament with a higher buckling force. A positive response prompted the use of next filament with a lower buckling force. This paradigm continued until 4 measurements were obtained, beginning with the one before the first change in response, or until five consecutive positive (assigned score 0.25 g) or negative (assigned score 15 g) measurements occurred.

Animals were tested for possible side effects observed as a reduction of righting, stepping, corneal and pinna reflexes as previously described. No apparent side effects of GZ4 were observed.

2.2.2. Transient channel transfection and electrophysiological recording

Human embryonic kidney (HEK)-293 cells (American Type Culture Collection, ATCC) were grown in Dulbecco's modified Eagle's medium (DMEM)-high glucose supplemented with 10% horse serum, 2 mM L-glutamine, 110 mg/l sodium pyruvate, 100 U/ml penicillin and 100 µg/ml streptomycin at 37 °C in a 5% CO₂/95% air humidified atmosphere. After splitting the cells on the previous day and seeding at 50–60% confluency, cells were transfected with the cDNA clones encoding recombinant Ca_v channel subunits.

Cell expression constructs were made by standard techniques, and their fidelity was verified by DNA sequencing. The α 1B-pKCRH2 construct containing the cDNA clone encoding the rabbit brain N-type Ca²⁺ channel Ca_v2.2 pore-forming subunit (GenBank accession number D14157)¹² was provided by Dr. B. Adams (Utah State University, USA). The cDNA coding the rat brain Ca_vα₂δ-1 (M86621)¹³ and the rat brain Ca_vβ₃ (M88751),¹⁴ provided by Dr. K. Campbell (University of Iowa, USA), were subcloned into the pcDNA3 vector (Invitrogen). The rat neuronal Ca_v1.3 (AF370009)¹⁵ was cloned into the pcDNA6/His vector (Invitrogen). HEK-293 cells were transiently transfected using Lipofectamine Plus transfection reagent (Invitrogen) as per the manufacturer's instructions using 1.6 µg of the cDNA clones encoding Ca_v channel subunits, together with 0.4 µg of the Green Lantern plasmid encoding GFP (Life Technologies). Two days after transfection, cells were briefly split at ~10% confluence and patch-clamp recording was performed ~4 h later from fluorescent cells. Likewise, HEK-293 cells stably expressing the Ca_v3.1a channel (AF190860)¹⁶ were grown as previously reported.¹⁷ For electrophysiological recordings, cells were lift-off plates, re-seeded on poly-L-lysine (0.05%)–precoated glass coverslips and used ~4 h after plating.

Whole cell patch-clamp recordings were performed as described previously.^{18,19} Currents were recorded at RT (22–24 °C) using Clampex 10 software and an Axopatch 200B amplifier (Molecular Devices), digitized at 5.71 kHz and filtered at 2 kHz. The resistance of the patch electrodes was 2–4 MΩ when filled with the internal solution. After establishing the whole-cell mode, capacitive transients were cancelled with the amplifier. Series resistance values were typically 2–10 MΩ, and no records were used in which the voltage error (as defined by $V_{er} = I_{max} \times R_a$) was >5 mV. Leak and residual capacitance currents were subtracted online by a standard P/4 protocol. Membrane capacitance (*C_m*) was determined as described previously and used to normalize currents.²⁰ Current recordings were obtained from individual cells and performed within the initial 15 min after breaking into the cells to minimize rundown. The recorded cells were preincubated with the drug for 1–3 h before electrophysiological recording. Differences in transfection efficiency/expression were avoided by co-transfecting the cells (in 1:4 dilution with respect

to the channel subunits) with a GFP construct, and recordings were made only in GFP expressing cells. Currents through Ca_v channels were recorded in the following extracellular solution (in mM): 120 tetraethylammonium chloride (TEA-Cl), 10 BaCl_2 , 10 4-(2-hydroxyethyl)-1-piperazine-ethanesulfonic acid (HEPES), and 10 glucose, with pH adjusted to 7.4 with TEA hydroxide (osmolality $\sim 300 \text{ mOsm kg}^{-1}$). The intracellular solution consisted of (in mM): 135 CsCl, 2 MgCl_2 , 10 HEPES, 4 MgATP, and 10 ethyleneglycol-bis-(β -aminoethylether)*N,N*-tetraacetic acid (EGTA), pH 7.1, osmolality $\sim 280 \text{ mOsm kg}^{-1}$.

GZ4 was dissolved in sterile distilled water (2.9 mM stock solution) and diluted to the desired concentration in the cell culture medium. HEK-293 cells expressing recombinant Ca_v channels were preincubated (1–3 h) with **GZ4** (500 μM) and then subjected to electrophysiological recordings.

3. Results

3.1. GZ4 synthesis

The synthesis of the novel GABA derivative (**GZ4**), which displays a close structure–activity relationship with gabapentinoid drugs, was achieved as shown in Figure 2. For the synthesis of the oxirane **2**, protoadamantanone **1** was used as starting material.^{21,22} This was converted to oxirane **2**, which was obtained as an inseparable mixture of epimers (*endo:exo* 1:15), as was evident from the ^1H NMR spectral data, upon treatment with dimethylsulfoxonium methylide. Ring opening of compound **2** with a solution of H_2SO_4 (0.085 M) in acetone afforded diol **3**.²³ Oxidation of diol **3** with Jones reagent under mild conditions afforded the desired ketoacid **4**.²⁴ Esterification of compound **4** gave ketoester **5**.²⁵ Reductive cyanation²⁶ of compound **5** was accomplished in high yield using toluenesulphonylmethyl isocyanide (TOSMIC) and yielded in cyanoester **6**; saponification of the latter afforded the desired cyanoacid **7**. Finally, hydrogenation of cyanoacid **7** over platinum oxide catalyst in ethanol at 55 p.s.i., in the presence of HCl (37%), gave the desired aminoacid **GZ4** in its hydrochloride form.

Since gabapentinoid drugs have been shown to reduce the functional expression of neuronal N-type ($\text{Ca}_v2.2$) channels, we examined the potential effects of the **GZ4** treatment initially on neuropathic pain relief in a rat model of neuropathic pain and then on recombinant $\text{Ca}_v2.2$ channels heterologously expressed in HEK293 cells.

3.2. GZ4 treatment in spinal nerve ligated rats blocks allodynia

We first tested whether spinal nerve ligation led to the development of neuropathic pain, by determining the sensitivity to von Frey filament stimulation at the plantar surface of the hindpaw

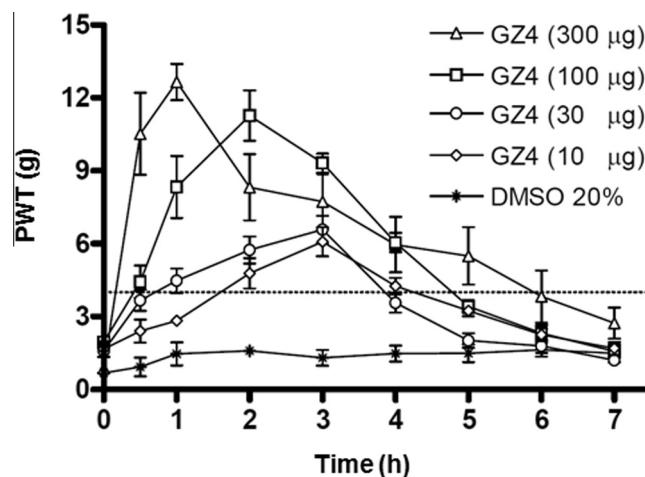


Figure 3. Effects of intrathecal GZ4 on spinal nerve ligation-induced allodynia. Animals with tactile allodynia were treated intrathecally with increasing doses ($\mu\text{g}/\text{rat}$) of **GZ4** or DMSO followed by the test for paw withdrawal thresholds (PWT) to von Frey filament stimulation as indicated. Data presented are the means \pm SEM from 6 rats in each group. * $P < 0.05$, by two-way repeated measures ANOVA.

of nerve ligated and sham animals. Our data indicated that the nerve ligation induced a gradual reduction in the hindpaw withdrawal threshold to the mechanical stimulation to a level considered allodynic (not shown). Data from our previous studies have shown that an adamantane derivative of GABA, AdGABA, produces strong inhibitory effects on whole-cell currents through neuronal N-type ($\text{Ca}_v2.2$) Ca^{2+} channels^{4,7} as well as on L-type channels of the $\text{Ca}_v1.3$ class,¹⁹ and exhibited analgesic activity on mice in the hot plate test.⁴ Hence, in order to investigate whether **GZ4**, a compound structurally related to AdGABA, has a potential analgesic activity, we injected the compound intrathecally in nerve ligated rats with allodynia followed by behavioral sensitivity assessment. Bolus **GZ4** treatment (10–300 μg) reversed allodynia in these animals, and its effects started 1 h after injection, peaked in 2 h, and diminished after 4 h of **GZ4** application (Fig. 3). Although it is difficult to estimate the concentration in the spinal cord, there is evidence that the therapeutic intrathecal doses of gabapentin in several studies are in the range of 10–300 μg . Thus, the concentrations of **GZ4** used in our study are similar to those reported to be effective for gabapentin.

3.3. GZ4 treatment inhibits macroscopic currents through recombinant Ca^{2+} channels in HEK-293 cells

To study whether a possible dysregulation of Ca^{2+} channel functional expression contributes to the development of allodynia at the

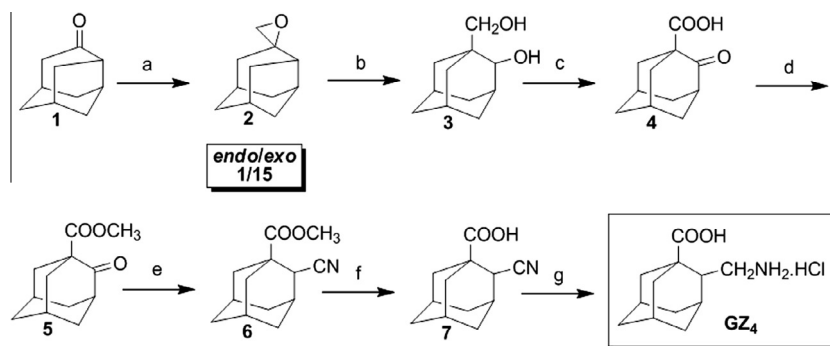


Figure 2. GZ4 synthesis. Reagents and conditions: (a) trimethylsulfoxonium iodide, NaH, DMSO, argon, 3 h 25 °C and then 8 h 55 °C; (b) H_2SO_4 (98%), H_2O , 75 min, reflux, (two steps yield: 60%); (c) Jones reagent (1 mM) (61%); (d) (i) SOCl_2 , 65 °C, 15 min, (ii) MeOH (quant); (e) TOSMIC, abs EtOH, DME, *t*-BuOK, 0 °C, argon, 30 min at 20 °C, and 1 h at 48 °C (81%); (f) EtOH, NaOH, H_2O , reflux, 2.5 h and then HCl (93%); (g) H_2/PtO_2 , EtOH, HCl, 50 p.s.i., 5 h (almost quantitative).

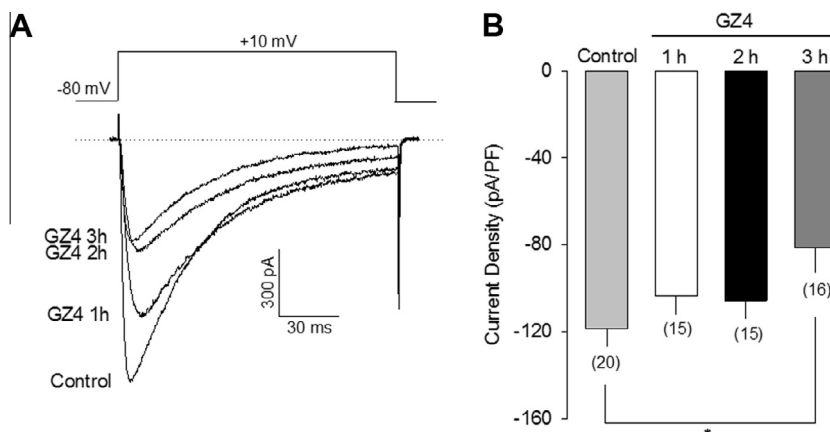


Figure 4. $\text{Ca}_v2.2$ channel current inhibition by GZ4 in HEK-293 cells. (A) Representative I_{Ba} traces under control conditions and inhibition in the presence of 500 μM GZ4 at different time points up to 3 h. (B) Bar chart showing data for mean current density through recombinant N-type Ca^{2+} channels ($\text{Ca}_v2.2\alpha_1/\text{Ca}_v\beta_3/\text{Ca}_v\alpha_2\delta-1$) expressed in HEK-293 cells measured at the peak of the inward current in response to a 140 ms voltage step command to 10 mV from a V_h of -80 mV. Data under control condition (Ctl) and in the presence of 500 μM GZ4 are shown. The number of recorded cells is shown in parenthesis and the asterisk denotes significant difference from the respective control ($*P < 0.05$, by Student's t -test).

spinal level of the nerve ligated rats, we next tested the effects of GZ4 on neuronal $\text{Ca}_v2.2$ channels heterologously expressed in HEK-293 cells. To this end, cells expressing the recombinant $\text{Ca}_v2.2$ channels ($\alpha_{1B}/\alpha_2\delta/\beta_3$) were kept in culture up to 3 h in the presence of 500 μM GZ4 prior to being subjected to electrophysiological recording. The results of this analysis showed a significant inhibition of $\text{Ca}_v2.2$ current density after drug treatment. The traces shown in Figure 4A illustrate representative whole-cell Ba^{2+} currents (I_{Ba}) through $\text{Ca}_v2.2$ channels elicited by 140 ms depolarizing pulses to +10 mV from a holding potential (V_h) of -80 mV in HEK-293 cells kept in a culture in the absence (control) and the presence of GZ4. Figure 4B shows that incubation of 1–2 h with GZ4 (500 μM) had a small effect on current density through recombinant $\text{Ca}_v2.2$ channels. In contrast, a significant inhibition of channel activity was observed after 3 h of drug treatment, supporting the notion that GZ4 may inhibit the functional expression of $\text{Ca}_v2.2$ channels.

Current inhibition was incomplete ($\sim 30\%$) with a GZ4 concentration of 500 μM , a value that is comparable to that obtained for GBP^{6,18} but greater than that observed with AdGABA.⁴ It should be noted, however, that AdGABA-induced inhibition of channel activity was observed upon chronic treatment (>24 h) with the drug, and that acute treatment (<8 h) had no significant effects on current amplitude.

Figure 5A shows the effect of GZ4 on I_{Ba} elicited in HEK-293 cells by depolarization to a wide range of voltages. As can be seen, treatment with GZ4 (3 h) inhibited inward currents at voltages ranging from -20 to $+30$ mV. Likewise, the participation of the $\alpha_2\delta$ subunit in the regulation of Ca_v channel voltage-dependent inactivation is well documented. This auxiliary subunit produces a hyperpolarizing shift in half-inactivation potential of Ca_v channels.^{19,27} Consistent with this, GZ4 treatment resulted in a significant change in the steady-state inactivation behavior of the Ca_v channels. Indeed, I_{Ba} in cells exposed to the drug exhibited an apparent ~ 10 mV hyperpolarizing shift in half-inactivation potential (Fig. 5B). The rightward shift in the prepulse inactivation curve could act to increase Ca^{2+} currents under physiological conditions. Hence, at a resting potential of -80 mV, there are more channel (about 5%) available to be open, although this is not sufficient to counteract the significant reduction of $\sim 35\%$ in maximum current observed after drug application. This finding may suggest that the inhibitory effect of the drug could be underestimated in our model system.

To corroborate role of the $\alpha_2\delta$ subunit in the GZ4-mediated regulation of N-type $\text{Ca}_v2.2$ channels, we next expressed recombinant channels with the α_{1B}/β_3 subunit composition in HEK-293 cells and tested the action of the drug. We observed that Ca^{2+} currents in

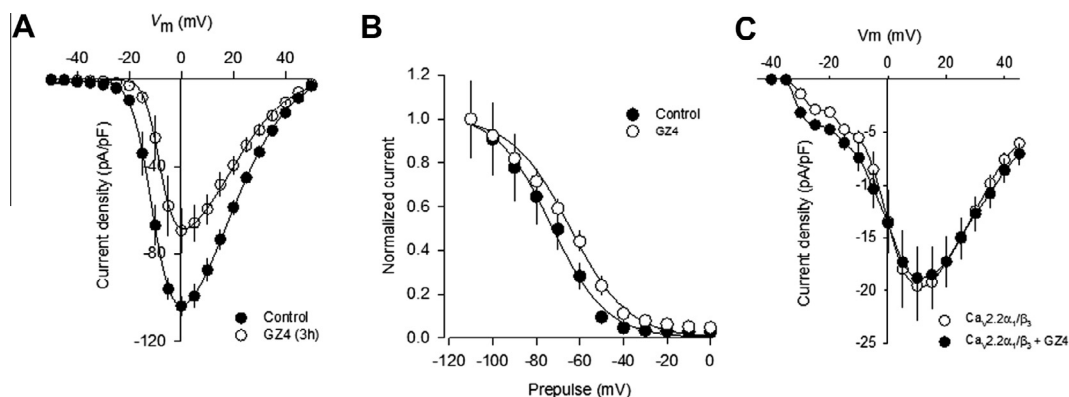


Figure 5. GZ4 treatment affects recombinant $\text{Ca}_v2.2$ current density and inactivation. (A) Current–voltage relationships for N-type Ca_v channel transfected cells ($\text{Ca}_v2.2\alpha_1/\text{Ca}_v\beta_3/\text{Ca}_v\alpha_2\delta-1$) in control conditions or after 3 h of treatment with 500 μM GZ4 ($n = 3-4$). (B) Voltage dependence of current inactivation. Currents were measured in transfected cells during depolarizations to +20 mV, preceded by 2 s inactivating pulses (prepulses) of various amplitudes applied from a V_h of -80 mV, in the absence and presence of the drug. Steady-state inactivation curves were fitted with a Boltzmann equation of the form: $I = I_{\text{max}} / [1 + \exp((V_{1/2} - V_m)/k)]$, where I_{max} represents the maximal current amplitude, $V_{1/2}$ the potential for half-maximal inactivation of I_{max} , and k is a slope factor. The resulting $V_{1/2}$ (mV) values for control and GZ4 treated cells were -73.1 and -67.1 , respectively ($n = 4-6$). (C) Current–voltage relationships for $\text{Ca}_v2.2\alpha_1/\text{Ca}_v\beta_3$ channel transfected cells (without $\text{Ca}_v\alpha_2\delta-1$) in control conditions or after 3 h of treatment with 500 μM GZ4 ($n = 6$).

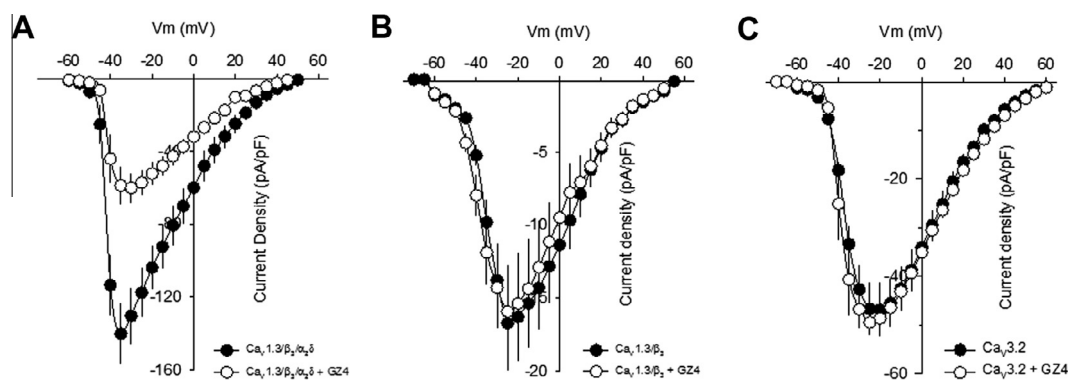


Figure 6. GZA treatment affects recombinant $\text{Ca}_V1.3$ but not $\text{Ca}_V3.1$ channel activity. (A) Current–voltage relationships for L-type Ca_V channel transfected cells ($\text{Ca}_V1.3\alpha_1/\text{Ca}_V\beta_3/\text{Ca}_V\alpha_2\delta-1$) in control conditions or after 3 h of treatment with 500 μM **GZA** ($n = 9$). (B) Current–voltage relationships for $\text{Ca}_V1.3\alpha_1/\text{Ca}_V\beta_3$ channel transfected cells (without $\text{Ca}_V\alpha_2\delta-1$) in control conditions or after 3 h of treatment with 500 μM **GZA** ($n = 5-7$). (C) Current–voltage relationships for T-type $\text{Ca}_V3.1$ channel transfected cells (without auxiliary subunits) in control conditions or after 3 h of treatment with 500 μM **GZA** ($n = 5-6$).

cells expressing α_{1B}/β_3 channels were substantially smaller (4–5-fold) than those in cells expressing $\alpha_2\delta$, and that the voltage dependence of activation was right shifted about 10 mV, what is expected for macroscopic currents through channels lacking the auxiliary subunit. Interestingly, the above mentioned effects of **GZA** on N-type $\text{Ca}_V2.2$ channel currents did not occur in the absence of the $\alpha_2\delta$ subunit. Ca^{2+} currents recorded in the control condition in HEK-293 cells transfected with $\text{Ca}_V2.2$ channels (α_{1B}/β_3) were of similar magnitude either in the absence or in the presence of **GZA** (Fig. 5C).

Previously, we showed that the co-expression of the $\alpha_2\delta$ subunit renders the $\text{Ca}_V1.3$ L-type channels sensitive to gabapentinoid drugs GBP and AdGABA.¹⁹ Therefore, we sought to determine whether these channels were also sensitive to the actions of **GZA**. To this end, we co-expressed the $\alpha_2\delta$ subunit and the $\text{Ca}_V1.3$ channels (α_{1D}/β_3) in HEK-293 cells and tested the effects of **GZA** (500 μM) after 3 h of incubation. Interestingly, **GZA** had a significant effect on peak L-type current amplitudes in cells expressing $\alpha_{1D}/\alpha_2\delta/\beta_3$ recombinant channels (Fig. 6A). Average peak L-type current density at -30 mV was -60.1 ± 8.3 in absence and -130.3 ± 15.3 pA/pF in presence of the drug. Consistent with the contribution of the $\alpha_2\delta$ subunit to this regulation, the inhibitory effects of **GZA** on L-type $\text{Ca}_V1.3$ channel currents were lost in the absence of the Ca^{2+} channel auxiliary subunit (Fig. 6B). Last, incubation (3 h) with the **GZA** (500 μM) had no effect on voltage-gated Ca^{2+} though T-type $\text{Ca}_V3.1$ channels stably expressed in HEK-293 cells used also as a negative control (Fig. 6C).

4. Discussion

Chronic pain is one of the most prevalent and disabling conditions in clinical practice. However, its therapeutic management is challenging. Diverse pharmacological options are available to manage different pain mechanisms including antidepressants, anticonvulsants opioid and topical analgesics.

Given that neuropathic pain is associated with changes in voltage-gated Ca^{2+} activity and expression, gabapentin and pregabalin are now been widely used in the treatment of pain. These two gabapentinoid drugs act as neuromodulators by selectively binding to the $\alpha_2\delta$ subunit of voltage gated Ca^{2+} channels in various regions of the brain and the dorsal horn of the spinal cord.²⁸ They also have a peripheral analgesic action.²⁹ These actions result in an inhibition of the release of excitatory neurotransmitters that are important in the production of pain. Likewise, several conotoxins are being investigated as antinociceptive drugs.³

Conotoxins are small peptides in the venom of tropical marine cone snails from the genus *Conus* that target ion channels including Na^+ and Ca^{2+} channels. Indeed, there is considerable interest in finding clinically relevant drugs to block Na^+ and Ca^{2+} channels involved in pain signaling.^{3,28} Despite the fact that several conotoxins have been tested in clinical trials, peptide toxins as drug leads have a few drawbacks, such as unstable disulfide bonds, protease degradation and inefficient transport to its intended site of action.³ Only the ω -conotoxin MVIIA from *Conus magus* has been approved as an analgesic drug (named Ziconotide) for severe chronic pain.^{28,30}

In the current report, we describe the synthesis of a GABA analog, **GZA**, with certain structure–activity relationship to gabapentin. By using a combined approach of spinal nerve ligation-induced neuropathic pain model as well as electrophysiological recordings and molecular biology, we show relevant aspects regarding the mechanism of action of this novel gabapentinoid drug. Our results show that this compound mimics some of the actions of GBP, i.e. inhibits N-type Ca^{2+} currents most likely acting on the $\alpha_2\delta$ subunit of the Ca_V channel complex heterologously expressed in HEK-293 cells. However, differences in the time courses of **GZA** and gabapentin action suggest divergences in their mode of action. It is acknowledged that gabapentin in vitro actions require at least 24 h and imply uptake of the drug, which suggests that gabapentin acts mainly intracellularly affecting channels trafficking to the plasma membrane.^{5,6} Indeed, recent studies have shown that GBP inhibits post-Golgi forward trafficking of the $\alpha_2\delta$ subunit in a manner that is prevented by dominant-negative construct of the small GTPase Rab11, which disrupts trafficking through the recycling endosome compartment. This finding indicates that GBP may disrupt the interaction between $\alpha_2\delta$ and sorting proteins in this compartment, and that this may represent a rate-limiting step in calcium channel trafficking.³¹ On the other hand, the faster time course (1–3 h) of **GZA** effect suggests a direct inhibition of Ca^{2+} currents through the alteration of the biophysical properties of cell surface channels. Our electrophysiological data support this hypothesis.

Although the reasons for the apparent differences in the time course of **GZA** and GBP action are currently unknown, they may lie in the structural differences. Gabapentin and AdGABA show similarities in the orientation in both the carboxymethylene and aminomethylene moiety. However, in the case of **GZA** the carboxylic acid group possessed a complete different orientation (Fig. 1B) and at the same time the two methylenes of the GABA moiety were introduced into the adamantane skeleton and adopted a very specific stereochemical orientation. This study demonstrates distinct

structure–activity relationships for the tested compounds, and therefore it is reasonable to speculate that the changes to the size and conformation of the GABA moiety had a significant effect on biological activity. Most probably, **GZ4** and gabapentin may be affecting differentially the tertiary structure of the receptor target (the Ca_v channel $\alpha_2\delta$ subunit). These are interesting topics for future studies.

It is also worth noting that high concentrations of **GZ4** (500 μ M; Figs. 4 and 5), as well as of GBP,^{5,6} are required to observe significant effects on I_{Ba} when recordings are made in single cells kept in culture. This may be related to the over-expression in the heterologous system of the Ca_v channel β auxiliary subunit which may change the binding properties of the channel complex. In addition, the possibility exists that the amino acids in the culture medium, may compete for the uptake of the gabapentinoids. However, the conditions present in the in vitro system differ significantly from those in vivo, in which the drug showed a more potent effect (Fig. 3).

In line with this, there have been a number of studies documenting the beneficial effects of gabapentinoid drugs in different models of neuropathic pain as well as in different types of neuropathic pain like neuropathy due to cancer, HIV infection, diabetic neuropathy, trigeminal neuralgia and post-operative neuropathic pain.³² In contrast to what has been described in vitro, the clinical assays show that gabapentinoids produce anti-allodynic effects \sim 1 h following oral administration.³³ This time course is consistent with the pharmacokinetic distribution of the compound. The disparity in results between the heterologous expression systems and the clinical studies may be due to several factors including channel subunit heterogeneity among native versus recombinant channels and in the pathologic state of the tissue that is, hyperalgesic or normal. In addition, it is worth noting that gabapentin has been shown to directly inhibit NMDA receptors and TRPA1 channels that might also be responsible for its anti-nociceptive activity.³²

Data from our behavioral testing showed that intrathecal **GZ4** application significantly reversed nerve ligation-induced tactile allodynia compared to that in allodynic rats treated with vehicle. While the underlying mechanisms of **GZ4** are unknown and still under investigation, our findings on the electrophysiological recording suggest that **GZ4** may act inhibiting the functional expression of N-type Ca²⁺ currents. Taken together, our results suggest that **GZ4** might serve as new therapeutic agent. It is possible that some benefits of the **GZ4** treatment may be of clinical significance, although this requires further investigation. The introduction of a mechanism-based drugs with a specific pharmacological action, may lead to more rational treatment for the patients with neuropathic pain.

Acknowledgments

This work was supported by funds from The National Council for Science and Technology (Conacyt, Mexico; Grants 128707; 179294) to R.F. and V.G.S., respectively, and from PAPIIT-UNAM (Grant IN221011) to A.S. A doctoral fellowship from Conacyt to J.B.P.F. is gratefully acknowledged.

References and notes

- Djoughri, L.; Fang, X.; Koutsikou, S.; Lawson, S. N. *Pain* **2012**, *153*, 1824.
- Adams, D. J.; Berecki, G. *Biochim. Biophys. Acta* **2013**, *1828*, 1619.
- Knapp, O.; McArthur, J. R.; Adams, D. J. *Toxins (Basel)* **2012**, *4*, 1236.
- Zoidis, G.; Papanastasiou, I.; Dotsikas, I.; Sandoval, A.; Dos Santos, R. G.; Papadopoulou-Daifoti, Z.; Vamvakides, A.; Kolocouris, N.; Felix, R. *Bioorg. Med. Chem.* **2005**, *13*, 2791.
- Vega-Hernandez, A.; Felix, R. *Cell. Mol. Neurobiol.* **2002**, *22*, 185.
- Hendrich, J.; Van Minh, A. T.; Heblich, F.; Nieto-Rostro, M.; Watschinger, K.; Striessnig, J.; Wratten, J.; Davies, A.; Dolphin, A. C. *Proc. Natl. Acad. Sci. U.S.A.* **2008**, *105*, 3628.
- Martínez-Hernández, E.; Sandoval, A.; González-Ramírez, R.; Zoidis, G.; Felix, R. *Toxicol. Appl. Pharmacol.* **2011**, *250*, 270.
- Zimmermann, M. *Pain* **1983**, *16*, 109.
- LoPachin, R. M.; Rudy, T. A.; Yaksh, T. L. *Physiol. Behav.* **1981**, *27*, 559.
- Chaplan, S. R.; Bach, F. W.; Pogrel, J. W.; Chung, J. M.; Yaksh, T. L. *J. Neurosci. Methods* **1994**, *53*, 55.
- Dixon, W. J. *Annu. Rev. Pharmacol. Toxicol.* **1980**, *20*, 441.
- Fujita, Y.; Mynlieff, M.; Dirksen, R. T.; Kim, M. S.; Niidome, T.; Nakai, J.; Friedrich, T.; Iwabe, N.; Miyata, T.; Furuichi, T.; Furutama, D.; Mikoshiba, K.; Mori, Y.; Beam, K. G. *Neuron* **1993**, *10*, 585.
- Kim, H. L.; Kim, H.; Lee, P.; King, R. G.; Chin, H. *Proc. Natl. Acad. Sci. U.S.A.* **1992**, *89*, 3251.
- Castellano, A.; Wei, X.; Birnbaumer, L.; Perez-Reyes, E. *J. Biol. Chem.* **1993**, *268*, 3450.
- Helton, T. D.; Xu, W.; Lipscombe, D. J. *Neurosci.* **2005**, *25*, 10247.
- Lee, J. H.; Daud, A. N.; Cribbs, L. L.; Lacerda, A. E.; Pereverzev, A.; Klöckner, U.; Schneider, T.; Perez-Reyes, E. *J. Neurosci.* **1999**, *19*, 1912.
- Avila, T.; Andrade, A.; Felix, R. *J. Cell Physiol.* **2006**, *209*, 448.
- Sandoval, A.; Andrade, A.; Beedle, A. M.; Campbell, K. P.; Felix, R. *J. Neurosci.* **2007**, *27*, 3317.
- Andrade, A.; Sandoval, A.; Gonzalez-Ramirez, R.; Lipscombe, D.; Campbell, K. P.; Felix, R. *Cell Calcium* **2009**, *46*, 282.
- Avila, G.; Sandoval, A.; Felix, R. *Cell. Mol. Neurobiol.* **2004**, *24*, 317.
- Majersky, Z.; Hamesrak, Z. *Org. Synth.* **1988**, *50*, 958.
- Kolocouris, N.; Zoidis, G.; Fytas, C. *Synlett* **2007**, 1063.
- Zoidis, G.; Benaki, D.; Myriantopoulos, V.; Naesens, L.; Clercq, E. D.; Mikros, E.; Kolocouris, N. *Tetrahedron Lett.* **2009**, *50*, 2671.
- Farcasiu, D. *J. Am. Chem. Soc.* **1976**, *98*, 5301.
- Peters, J. A.; Van Der Toorn, J. M.; Van Bekkum, H. *Tetrahedron* **1975**, *31*, 2273.
- Oldenziel, O.; Van Leusen, D.; Van Leusen, A. J. *Org. Chem.* **1977**, *42*, 3114.
- Felix, R.; Gurnett, C. A.; De Waard, M.; Campbell, K. P. *J. Neurosci.* **1997**, *17*, 6884.
- Pexton, T.; Moeller-Bertram, T.; Schilling, J. M.; Wallace, M. S. *Expert Opin. Invest. Drugs* **2011**, *20*, 1277.
- Carlton, S. M.; Zhou, S. *Pain* **1998**, *76*, 201.
- Miljanich, G. P. *Curr. Med. Chem.* **2004**, *11*, 3029.
- Tran-Van-Minh, A.; Dolphin, A. C. *J. Neurosci.* **2010**, *30*, 12856.
- Kukkar, A.; Bali, A.; Singh, N.; Jaggi, A. S. *Arch. Pharm. Res.* **2013**, *36*, 237.
- Schmidt, P. C.; Ruchelli, G.; Mackey, S. C.; Carroll, I. R. *Anesthesiology* **2013**, *119*, 1215.